



DOI: 10.15593/perm.mech/eng.2018.1.11

UDC 691.32:620.178.73

## FRACTAL ANALYSIS OF DEFORMATION CURVES OF DISPERSE REINFORCED FINE-GRAINED CONCRETE UNDER COMPRESSION

V.P. Selyayev, T.A. Nizina, A.S. Balykov, D.R. Nizin, A.V. Balbalin

Ogarev Mordovia National Research University, Saransk, Russian Federation

### ARTICLE INFO

Received: 16.11.2015

Accepted: 17.02.2016

Published: 30.06.2018

#### Keywords:

deformation curves, composite construction materials, dispersed reinforcement, fine-grained concrete, the minimal covering method, the Hurst method, fractality index, fractal dimension, fracture path parametric points

### ABSTRACT

The paper describes the methodology of fractal dimension definition for deformation curves on the basis of the minimal covering method. The methodology allows to obtain the integral quantitative estimation of fracture of structural composite materials under compression and define the location of the fracture path parametric point. We compared the offered method to the algorithms for definition of the Hurst exponent and fractal dimension by the square covering method. The work shows the advantage of the methodology based on definition of the fractal dimension using the minimal covering method.

To perform the mechanical testing of dispersal reinforced fine-grained concrete compositions, we used the WilleGeotechnik® hardware and software system additionally equipped with a climatic chamber allowing for temperature (from  $-40$  to  $+100$  °C) and humidity (from 10 to 96 %) adjustment during the loading. The change of stress and deformations of the samples during the loading was registered spaced at 0.01 sec.

We used the following materials as the main components of disperse reinforced fine-grained concrete: CEM I 42.5B concrete, gravel sand, condensed and densified microsilicasuspension MKU-85, polycarboxylate superplasticizing agent Melflux 1641 F. Dispersed reinforcement of concrete was ensured by a separate adding of three types of fiber, i.e. the polypropylene multifilament fiber, polyacrylonitrile synthetic fiber FibARM Fiber WB and astralene modified basalt microfiber Astroflex-MBM.

We defined the values of indices of fractality and fractal dimension of stress incrementation and deformations of deformation curves for fine-grained concrete using the minimal covering method. On the basis of the fractal analysis of dynamic series, we defined the location and vicinity of the point of transition from the quiescent condition to the apparent trend for the concrete sample. We revealed the change of location of the parametric point and fractal dimension values depending on the type of fiber. It was discovered that the incorporation of 1 % of the polypropylene multifilament fiber or 5 % of the astralene modified basalt microfiber Astroflex-MBM resulted in the substantial increase of the first critical level, up to 54 and 47 % accordingly, both in the stress incrementation and deformation analyses compared to 19 and 28 % for the compositions containing 1.5 % of the polyacrylonitrile synthetic fiber.

The proposed methodology of the fractal analysis of deformation curves on the basis of the minimal covering method allows to obtain valuable information about the fracturing process of different composite materials.

© PNRPU

© **Vladimir P. Selyaev** – Academician of the RAACS, Doctor of Technical Sciences, Professor, e-mail: [ntorm80@mail.ru](mailto:ntorm80@mail.ru)

**Tatyana A. Nizina** – Doctor of Technical Sciences, Professor, e-mail: [nizinata@yandex.ru](mailto:nizinata@yandex.ru)

**Artemy S. Balykov** – Ph. D. student, e-mail: [artbalrun@yandex.ru](mailto:artbalrun@yandex.ru)

**Dmitriy R. Nizin** – Ph. D. student, e-mail: [nizindi@yandex.ru](mailto:nizindi@yandex.ru)

**Alexey V. Balbalin** – Ph. D. student, e-mail: [06.89@mail.ru](mailto:06.89@mail.ru)



## Introduction

It is known that fracturing of composite materials, including cement concrete and grout, is a process of multiple nucleation, growth, and aggregation of different defects and microcracks up to the generation of macrocracks. Today it is beyond argument that the structural discontinuity of cement composites generates weak areas, where the material begins to loose up and fracture. The analysis of the concrete fracture mechanism as the process of progressive fracture of integrity was proposed in the works of A.A. Gvozdev, O.Ya. Berg, Yu.V. Zaytzev, N.I. Karpenko and other researchers [1-3].

The process of concrete fracturing under the action of forces begins at the microscale level as a discrete advance action of a primary microcrack to a pore or a filler particle. When the microcrack reaches an inclusion (a pore or a filler particle), the energy of critical density discharges to the mouth of the crack and the system enters an unstable condition (the bifurcation point). At the bifurcation point, the fracture crack can branch, change its development mechanism or direction. The fracture process of the sample consists of discrete fracture actions at the microscale level [4]. In addition to the above, the fracturing has a stochastic nature and the process of damage accumulation is self-similar that allows us to use the fractal theory [5].

Academic literature describes different ways to define fractal dimension of structure of real composite materials with cement and plastic binders [6-10]. It was defined that the fractal analysis for the quantitative evaluation of structure inhomogeneity of polymer materials and pore structure of cement composite materials allows to find a compact way to describe similar objects. The works propose the modified methods to define fractal dimension of filled polymer composites according to the length of the section and the size of the surface area. These methods are more convenient and easy to perform compared to the traditional square covering method [6, 8].

The works [11, 12] describe the application results of the fractal calculation methods for the evaluation of growth of fatigue cracks in metal. The process of nucleation and development of fatigue cracks in titanium alloys, using the method of infrared thermography under cyclic load, was studied with the help of the fracture surface analysis [11], as well as localization of deformations during a high-speed deformation and development of fatigue cracks under gigacyclic load in the aluminum and magnesium alloy AMr6 [12].

The software of the modern testing equipment is a high-precision system for collection and registration of the results adapted to receive large amount of data. Registration of change in the load and deformation of the sample during the load can be spaced not merely at a fraction of a minute but also at a fraction of a second [4]. Depending on the test conditions using modern testing systems, the load speed may be set in the form of a constant value characterizing the stress or deformation buildup with time that allows to use

the theory of fractal analysis of dynamic series. Such dynamic series include a wide range of different processes: from stochastic (the Brownian agitation) to deterministic [13-16]. The commonness of fractal properties of dynamic series speaks for a universal mechanism leading to fractality in completely different real systems.

## 1. Equipment and Methodology of Defining Fractal Dimension of Deformation Curves

In this work we used the hardware and software system WilleGeotechnik® (the model 13-PD/401) to perform mechanical tests of dispersal reinforced fine-grained concrete compositions. The system is additionally equipped with a climatic chamber allowing for temperature and humidity adjustment during the loading. The system allows to perform tests and monitor their parameters on the real-time basis and includes a high-precision system with the resolution above 1.000.000 steps (20 bit), 3 freely switchable channels for each axis (stress, translation, pressure) and the possibility to connect up to 16 additional measuring channels. The climatic chamber allows to perform researches within the range of temperature from  $-40$  to  $+100$  °C and humidity limits of 10-96 %. Settings adjustment and processing of the acquired data were performed with the help of the GEOSYS 8.7.8 software. Change of stress and deformation of the composite materials during the load were registered with the step of 0.01 sec and the load speed of 2 mm/min (Fig. 1, a).

When tracing the fragments of the deformation curve on a large scale, one can clearly see (Fig. 1, b) that the process of deformation buildup is accompanied by discrete rises and falls of stress. Also, for a variety of the deformation diagram parts we can see increase and decrease of relative deformation with no substantial stress incrementation. Taking into account that stress and deformation incrementation in the sample under mechanic tests, using the WilleGeotechnik® hardware and software system, develop with time and a certain set step (0.01 sec), we apply the theory of fractal analysis of dynamic series to analyze the deformation curves.

Let us consider the determination method of fractal structure of dynamic series  $y(t)$ . Suppose  $\Delta$  is the vicinity of the point  $t \in [0, T]$ . Then the fractal dimension of the function  $y(t)$  on the interval  $[t - \Delta, t + \Delta]$ , defined using the square covering method with the side of the squares of  $\delta < \Delta$ , is determined from the formula:

$$D(\Delta, t) = \lim_{\delta \rightarrow 0} \frac{N(\delta)}{\ln\left(\frac{1}{\delta}\right)} = 1 + \lim_{\delta \rightarrow 0} \frac{\ln(A(\delta))}{\ln\left(\frac{1}{\delta}\right)}, \quad (1)$$

where  $N(\delta)$  is the quantity of the squares with the side of  $\delta$  covering the function graph  $y(t)$  on the interval  $[t - \Delta, t + \Delta]$ .

$A(\delta)$  is the size of the covered area, determined as  $A(\delta) = N(\delta) \times \delta$ .

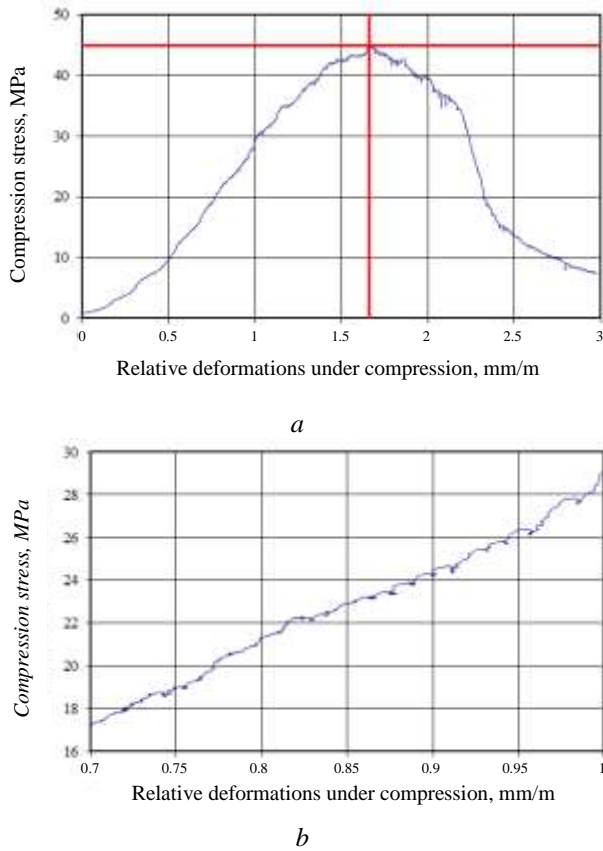


Fig. 1. General view (a) and a fragment (b) of the deformation curve of composition of disperse reinforced fine-grained concrete under compression

Fractal dimension  $D(\Delta, t)$  is an integral characteristic of the function on the interval  $[t - \Delta, t + \Delta]$ , depends on the length of the interval  $\Delta$  and is available for any continuous function  $y(t)$ . If the function is continuously differentiable, then [17]:

$$\lim_{\delta \rightarrow 0} \frac{\ln(A(\delta))}{\ln\left(\frac{1}{\delta}\right)} = 0 \text{ and } D(\Delta, t) = 1.$$

Consequently, if  $D(\Delta, t) > 1$ , then it speaks for the fractal structure of the considered time process.

Let us choose from the interval  $[t - \Delta, t + \Delta]$  an assembly of points  $t_0 = t - \Delta < t_1 < \dots < t_n = t + \Delta$  and define the length of the polygonal curve

$$L_n \sum_{i=1}^n l_i, \tag{2}$$

connecting consequent points by linear segments  $(t - \Delta, y_0), (t_1, y_1), \dots, (t + \Delta, y_n)$ , where  $l_i$  is the length of the segment on the plane  $y(t) - t$ , connecting the points  $(t_{i-1}, y_{i-1}), (t_i, y_i)$  that is calculated according to the following formula:

$$l_i = \sqrt{(t_i - t_{i-1})^2 + (y_i - y_{i-1})^2}. \tag{3}$$

In the case if the decomposition grid of the interval is equally spaced  $[t - \Delta, t + \Delta]$ , we have

$$t_i = t_{i-1} + \delta.$$

Assume that the number of points increases with no limit ( $n \rightarrow \infty$ ), so  $\delta \rightarrow 0$ . If the function has no fractal structure, then

$$\lim_{\delta \rightarrow 0} L_n(\delta) = L,$$

where  $L$  is the length of the curve corresponding to the function graph  $y(t)$ .

Assume that the function  $y(t)$  is such that  $L_n(\delta) \rightarrow +\infty$  at  $\delta \rightarrow +0$  provided that

$$L_n(\delta) \sim \delta^{-\gamma}; \quad \gamma > 0; \quad \delta \rightarrow 0. \tag{4}$$

Then the function  $y(t)$  has a fractal structure and the value  $\gamma > 0$  is its criterion and defines the degree of fractal structure: the larger the value  $\gamma$ , the larger the degree of fractal structure of the function. The value  $\gamma$  is referred to as the length index and is calculated in the following way

$$\gamma = \lim_{\delta \rightarrow 0} \frac{\ln(L(\delta))}{\ln\left(\frac{1}{\delta}\right)}. \tag{5}$$

Geometrically the length index is interpreted as a tangent of the straight line slope in double logarithmic scale with small  $\delta > 0$ :

$$\ln(L(\delta)) = a + \gamma \cdot \ln\left(\frac{1}{\delta}\right). \tag{6}$$

The definition of fractal dimension of the function  $y(t)$  suggests, that the function should be defined in all point set of the interval  $[t - \Delta, t + \Delta]$ . However, dynamic series in many technical fields form sequences  $y_i$ , where the index  $i = 1, \dots, n$  points to discrete time tagging which have known values of the time interval.

Let us consider a discrete time process in the form of a dynamic series

$$y_1, \dots, y_n. \tag{7}$$

We brake the totality of numbers  $i = 1, \dots, n$  to groups with the divider  $m_1$ :

$$\begin{aligned} j = 1 &: i = 1, \dots, m_1; \\ j = 2 &: i = m_1 + 1, \dots, 2 \cdot m_1, \\ j = n_1 &: i = (n_1 - 1) \cdot m_1 + 1, \dots, n_1 \cdot m_1, \end{aligned}$$

where  $n_1 = \left\lfloor \frac{n}{m_1} \right\rfloor$ .

In the same way we brake the totality of numbers  $i = 1, \dots, n$  to  $n_2$  groups  $\left( n_2 = \left\lfloor \frac{n}{m_2} \right\rfloor \right)$  with the divider  $m_2$

etc. up to  $m_k$ . Let us consider an alternative for the length index  $\gamma$ , defined for the function of continuous argument by the equation (5), for a discrete dynamic series. We connect nearest sequences of points by

$$(0, y_1), \left(\frac{m_1}{n}, y_{m_1}\right), \left(\frac{2m_1}{n}, y_{2m_1}\right), \dots, \left(\frac{(n_1-1) \cdot m_1}{n}, y_{(n_1-1) \cdot m_1}\right), \left(\frac{n_1 \cdot m_1}{n}, y_{n_1 \cdot m_1}\right)$$

linear segments.

Let us set  $L(m_i)$  as the length of the polygonal curve connecting pairs of adjacent points in series. Then accordingly we have for  $m_1, m_2$  and  $m_k$  the following:

$$L(m_1) = \sum_{i=1}^{n_1} \sqrt{\frac{m_1^2}{n^2} + (y_{im_1} - y_{(i-1)m_1})^2};$$

$$L(m_2) = \sum_{i=1}^{n_2} \sqrt{\frac{4m_1^2}{n^2} + (y_{im_2} - y_{(i-1)m_2})^2};$$

...

$$L(m_k) = \sum_{i=1}^{n_k} \sqrt{\frac{m_1^2 n_k^2}{n^2} + (y_{im_k} - y_{(i-1)m_k})^2}.$$

It is obvious that the following inequations are correct

$$L(m_k) < L(m_{k-1}) < \dots < L(m_1).$$

Then we define the length index of the discrete dynamic series (7) as the tangent of slope of the straight line in double logarithmic scale  $\ln(m) - \ln(L(m))$ .

Today the Hurst method is the most abundantly used method for the determination of fractal dimension of dynamic series. However, the original calculation method for the Hurst exponent  $H$  using  $R/S$  is quite cumbersome, therefore the power law is often used to define it [17, 18]:

$$\langle |X_{i+\delta} - X_i| \rangle \sim \delta^H. \tag{8}$$

In addition, the value of the Hurst exponent is defined as the slope coefficient of the function graph  $f(\delta) = \langle |X_{i+\delta} - X_i| \rangle$  created in double logarithmic scale. The main disadvantage of this method is the need for experimental definition of a large amount of data as well as quite a slow output to asymptotics during the analysis of real fractal structures [17, 18].

The work [19] proposes a numerical algorithm for definition of the local fractal dimension of dynamic series on the basis of the sequence of approximations that allow to quickly find the output of the function to the asymptotic mode

$$S(\delta) \sim \delta^{2-D} \text{ under } \delta \rightarrow 0. \tag{9}$$

If we rearrange the equation

$$D = \lim_{\delta \rightarrow 0} \frac{\ln(N(\delta))}{\ln\left(\frac{1}{\delta}\right)}, \tag{10}$$

multiply its two parts by  $1/\delta$  and bring  $D$  to a logarithm, we obtain the following:

$$N(\delta) \sim \delta^{-D} \text{ under } \delta \rightarrow 0. \tag{11}$$

If now we multiply the two parts (11) by  $\delta^2$ , then the equation for definition of fractal dimension can be written over as a power function (9) using the approximation surface  $S(\delta)$ .

Let us consider the dynamic series  $y(t)$  defined on a certain interval  $[a, b]$ . To calculate fractal dimension, we used the minimal covering method that is more precise than the cellular dimension method. Fundamental principles of the minimal covering method are described in the works [19–21]. The principle of the method involves the proportional partition of an interval

$$\omega_m = [a = t_0 < t_1 < \dots < t_m = b]$$

to  $m$  parts and calculation of the function  $y = f(t)$  in the class of surfaces consisting of rectangles with the base of

$$\delta = \frac{b-a}{m} \text{ (Fig. 2 [19]). Then the height of a rectangle on}$$

the interval  $[t_{i-1}, t_i]$  equals to the difference of the maximum and minimum value of the function  $f(t)$  on this interval –  $K_i(\delta)$ . If we introduce the amplitude fluctuation value of the function  $f(t)$  corresponding to the scale of partition  $\delta$  on the interval  $[a, b]$

$$V_f(\delta) = \sum_{i=1}^m K_i(\delta), \tag{12}$$

we obtain the functional connection to find the full size of the covered area:

$$S_\mu(\delta) = V_f(\delta) \cdot \delta. \tag{13}$$

According to (1), it follows that

$$V_f(\delta) \sim \delta^{-\mu} \text{ under } \delta \rightarrow 0, \tag{14}$$

where  $\mu$  is the fractality index connected to dimension of the minimal covering  $D_\mu$  as

$$\mu = D_\mu - 1. \tag{15}$$

To compare the fractal dimension  $D_\mu$ , defined by the minimal covering method, to the cellular dimension  $D_c$ , let us consider cellular partition of the function graph plane  $f(t)$  (see Fig. 2). Assume that  $N_i(\delta)$  is the number of cells covering the function graph  $f(t)$  inside the interval  $[t_{i-1}, t_i]$ . Then Figure 2 shows that

$$0 < N(\delta) \cdot \delta^2 - K_i(\delta) \cdot \delta < 2\delta^2. \tag{16}$$

We divide this formula by  $\delta$ , sum over all  $i$ , taking into account (12), and obtain the following

$$0 < N(\delta) \cdot \delta - V_f(\delta) < 2(b-a), \tag{17}$$

where  $N(\delta) = \sum N_i(\delta)$  is the total number of cells with the size of  $\delta$  covering the function graph  $f(t)$  on the interval

[*a*, *b*]. We pass on to the limit under  $\delta \rightarrow 0$ , taking into account (14) and (15), and we have

$$N(\delta) \cdot \delta \sim V_f(\delta) \sim \delta^{-\mu} = \delta^{1-D_\mu}. \quad (18)$$

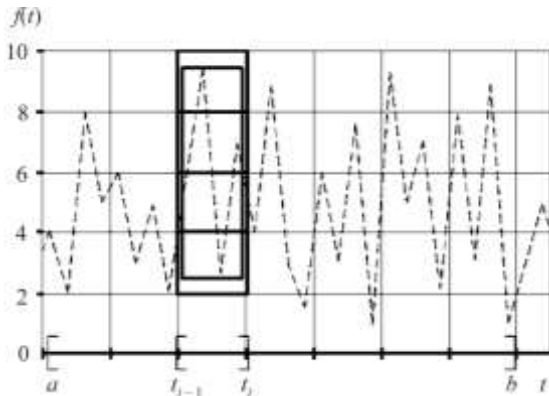


Fig. 2. The fragment of cellular (squares) and minimal (rectangles) covering of the fractal function graph on the interval [ $t_{i-1}$ ,  $t_i$ ]

On the other hand, according to the equation (10)

$$N(\delta) \cdot \delta = S_c(\delta) \cdot \delta^{-1} \sim \delta^{-1-D_c}. \quad (19)$$

Consequently  $D_c = D_\mu$ .

Taking into account that the minimal covering method for the analysis of dynamic series is simpler for operation and gives a faster output to the asymptotic mode, we will use it for the fractal analysis of deformation curves of dispersal reinforced concrete under compression.

## 2. Materials Employed

We used a portland cement class CEM I 42.5B, produced by OAO “Mordovcement”, to obtain compositions of fine-grained fibred concrete with multipurpose modifying additives. We used gravel sand with grain size less than 5 mm as a fine-grained filler produced in the town of Smolnii of the Ichalkovsk district, the Republic of Mordovia. Percentage of the fine-grained filler reached 65 % of the solid state mass.

Dispersed reinforcement of the concrete was ensured by a separate adding of three types of fiber in the amount of 1; 1.5 and 5 % of the binder mass accordingly:

1. The low-modulus polypropylene multifilament fiber with the cut length of 12 mm, diameter of 25-35 micron, the density of 0.91 g/cm<sup>3</sup>;

2. The high-modulus polyacrylic synthetic fiber with special treatment for concrete FibARM Fiber WB with the cut length of 12 mm, diameter of 14-31 micron, density of 1.17-0.03 g/cm<sup>3</sup>;

3. The astralene modified basalt microfiber under the brand name Astroflex-MBM FibARM Fiber WB with the length of 100-500 micron, average diameter of 8÷10 micron, bulk density of 800 kg/m<sup>3</sup>, with astralene content of 0.0001-0.01 % of the fiber mass.

To perform the multifunctional modification of the fine-grained concrete, we used condensed and densified

microsilicasuspension (MKU-85), produced by OAO “Kuznetzkiye Ferrosplavy”, in the amount of 20 % of the cement mass. To ensure required rheological properties, we used the polycarboxylate superplasticizing agent Melflux 1641 F (BASF Constraction Polymers, Germany) in the amount of 0.5 % of the binder mass.

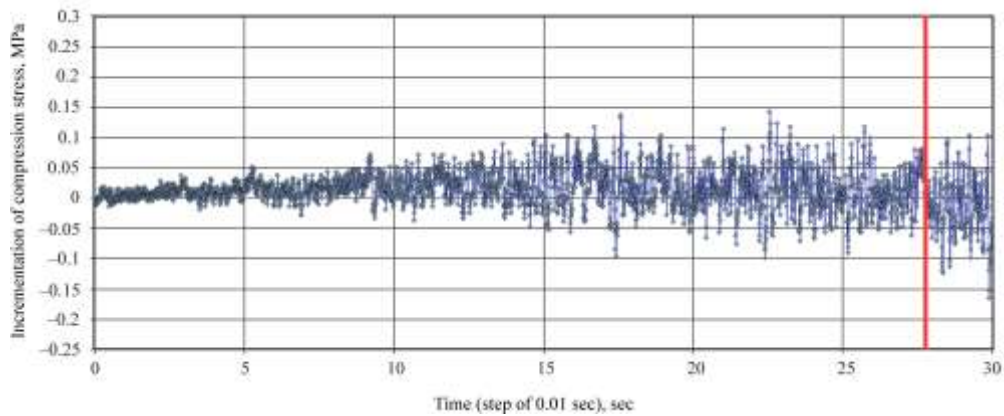
## 3. Fractal Analysis of Deformation Curves under Compression

Let us perform the analysis of deformation curves of dispersal reinforced fine-grained concrete compositions to the fracture point with the help of the minimal covering method representing data in the form of dynamic series that describe incrementation of stress during the loading process (Fig. 3) and relative deformation with different steps (0.01, 0.04, and 0.16 sec). To define the fractality index  $\mu$ , we used the nested partition sequence  $m$  where  $m = 2^n$  and  $n = 0, 1, 2, \dots, 12$ . Each partition consisted of  $2^n$  intervals containing  $2^{12-n}$  experimental points. For each partition  $\omega_m$  we calculated the amplitude fluctuation  $V_f(\delta)$  according to the formula (12), where  $K_i(\delta)$  was defined as the difference between the maximum and minimum stress (deformation) incrementation under compression on the time interval [ $t_{i-1}$ ,  $t_i$ ]. The analysis of Fig. 4 shows that the processed data correspond strictly to a straight line. Using the coefficient  $a$  of the regression equation  $y = ax + b$  calculated by the least square method, we defined the fractality index and dimension of the minimal covering:

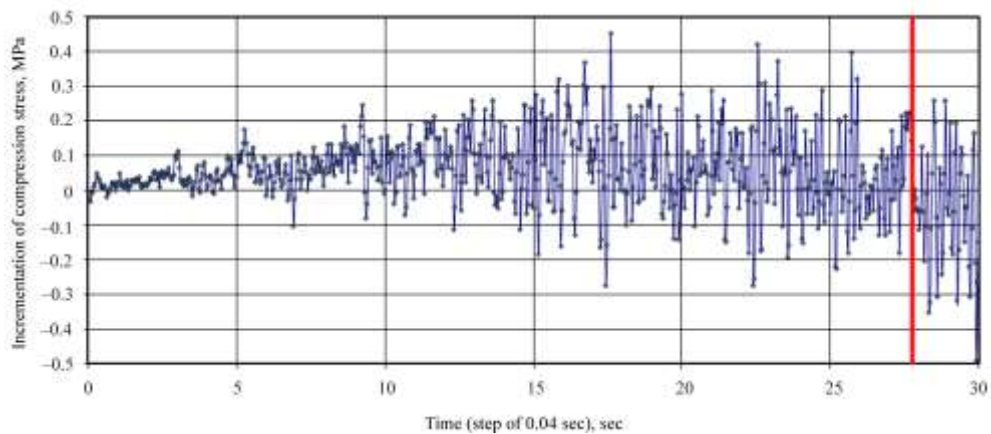
$$\mu = -a; D_\mu = 1 + \mu.$$

Fractality indices of the deformation curve for the incrementation analysis of stress and deformation of the reference fine-grained concrete composition, defined according to Fig. 4, equal to  $\mu_\sigma = 0,638$  and  $\mu_\epsilon = 0,789$ ; dimension of the minimal covering equals to  $D_{\mu_\sigma} = 1,638$  and  $D_{\mu_\epsilon} = 1,789$  accordingly. Values of fractal dimension for the concrete compositions containing three types of fiber are listed in the Table 1. Determination coefficients  $R^2$  vary in the interval of 0.982-0.996 that supports high integrity of the obtained data approximation by the linear model.

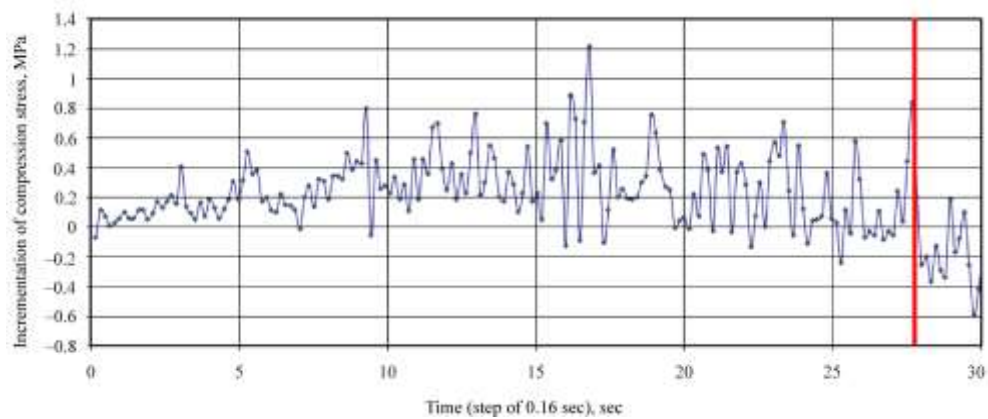
The obtained results show that it is practical to use the fractality indices  $\mu_\sigma$  and  $\mu_\epsilon$  of the fracture path, calculated using the minimal covering method, as a local characteristic defining dynamics of the loading process. To describe condition of a composite construction material in the process of deformation, we need to refer the value  $\mu$  to the behavior of the series that we analyze, i.e. to introduce the function  $\mu(t)$  as the value  $\mu$  defined on the minimum, preceding  $t$ , interval  $\tau_\mu$ . If the argument  $t$  is continuous, we choose an arbitrary small interval [19–21]. In our case, as the obtained dynamic series is spaced at 0.01 sec, we choose the interval containing  $2^4 = 16$  points  $\tau_\mu = 0,16$  sec. The calculation results are shown in Fig. 5.



a



b



c

Fig. 3. Dynamic series of stress incrementation according to the step of readings: a – 0.01; b – 0.04; c – 0.16 sec (the vertical line denotes the moment when the sample fractures)

Let us analyze the change of the stress incrementation fractality index, shown in Fig. 5, a, from the perspective of the dynamic series analysis. It is known [18] that the bigger the value  $\mu$ , the more stable the series. If  $\mu < 0.5$ , the series is interpreted as a trend (the period of relatively sustained up or down motion); if  $\mu > 0.5$ , the series is interpreted as a flat (the period of a relative stillness). If  $\mu \approx 0.5$ , we can say that these changes correspond to the Brownian agitation. The analysis of the Fig. 5, a shows that

the sample of fine-grained concrete changes its condition from flat to trend in 10.4 sec after the deformation begins. This time point of the deformation curve corresponds to 31 % of the fracture stress and 37 % of the maximum deformation (Fig. 5, c). The values of the determination coefficient  $R^2$  for the linear dependences, used to define the fractality index  $\mu$ , vary within the interval of 0.98-0.997 (Fig. 5, b) that confirms accuracy of the minimal covering method we used.

Table 1

Values of the fractality index and fractal dimension of deformation curves of dispersal reinforced fine-grained concrete under compression

Number of composition	Type of fiber	Fractality index				Fractal dimension	
		$\mu_\sigma$	$R^2$	$\mu_\varepsilon$	$R^2$	$D_{\mu_\sigma}$	$D_{\mu_\varepsilon}$
1	type 1	0.681	0.982	0.799	0.993	1.681	1.799
2	type 2	0.665	0.988	0.743	0.996	1.665	1.743
3	type 3	0.657	0.991	0.793	0.994	1.657	1.793

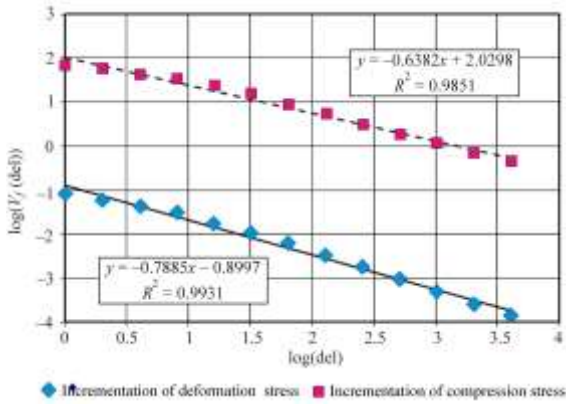
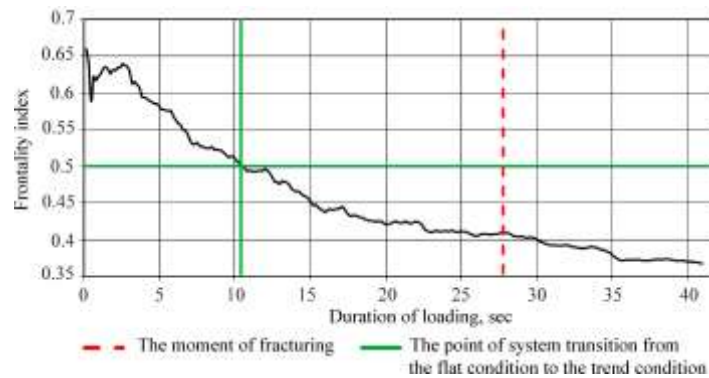
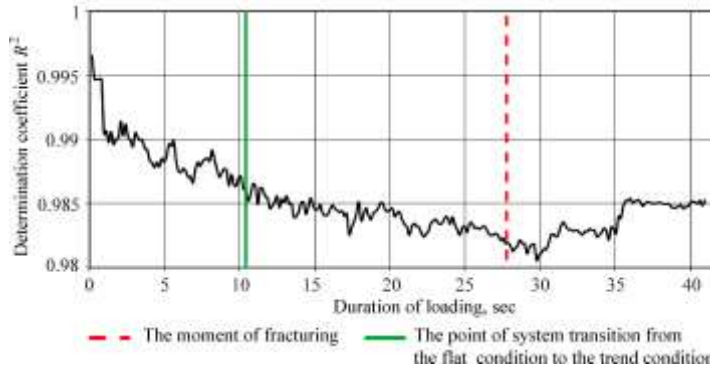


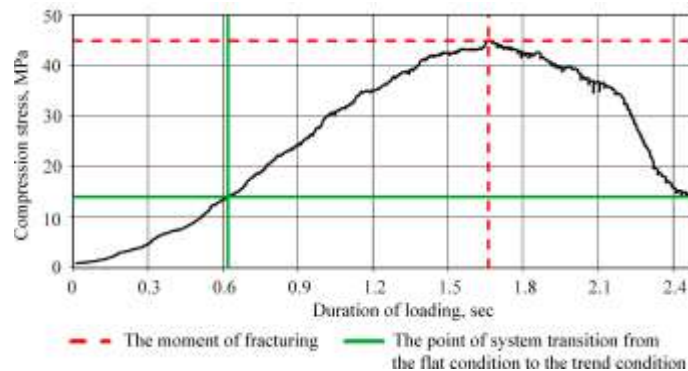
Fig. 4. Change of the variations amplitude depending on the approximation step of deformation curves of the reference fine-grained concrete composition under compression in double logarithmical coordinates



a



b



c

Fig. 5. Change of the fractality index (a) and determination coefficient (b) of stress incrementation of the deformation curve (c) of the reference fine-grained concrete composition depending on duration of loading (the vertical dashed line is the fracturing time of the sample, the vertical solid line is the point of condition transfer of the sample to the intermediate state between the flat and trend, the horizontal solid line corresponds to  $\mu = 0,5$ )

The main parameters of the fracture moment and the point of transition of the dispersal reinforced fine-grained concrete samples from the flat condition to the trend condition are listed in Table 2. We propose to use these values as numeric coordinates of the fracture process parametric point that speaks for accumulation of a certain level of microdefects in the volume of the composite material that leads to first cracks.

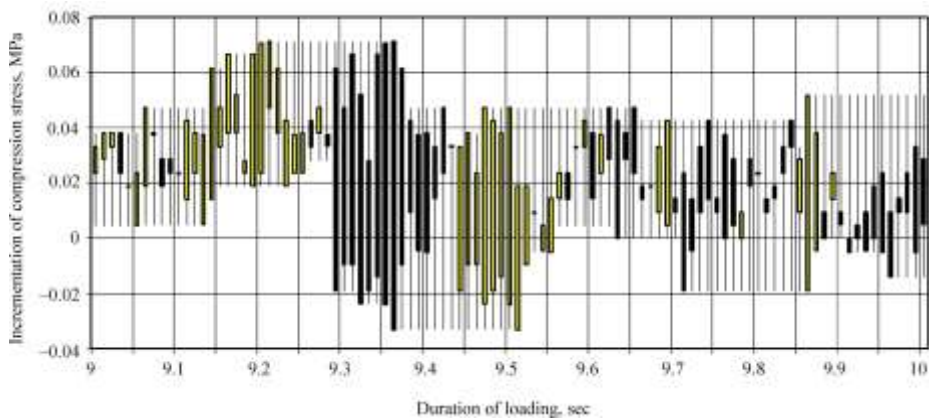
Let us perform the analysis of the vicinity of the point of transition of the concrete sample from a relatively

quiescent condition to the apparent trend on the basis of characteristic curves in the form of Japanese candlesticks charting (Fig. 6). Generally, this type of charts is used for the analysis of price movement involving 4 types of data: the opening price, the maximum and minimum price, the closing price [22]. For purposes of the deformation curve analysis, these 4 columns of data will contain the following: the stress (or deformation) incrementation in the starting point of the time interval, the maximum and minimum of the value that we analyze, the stress incrementation in the

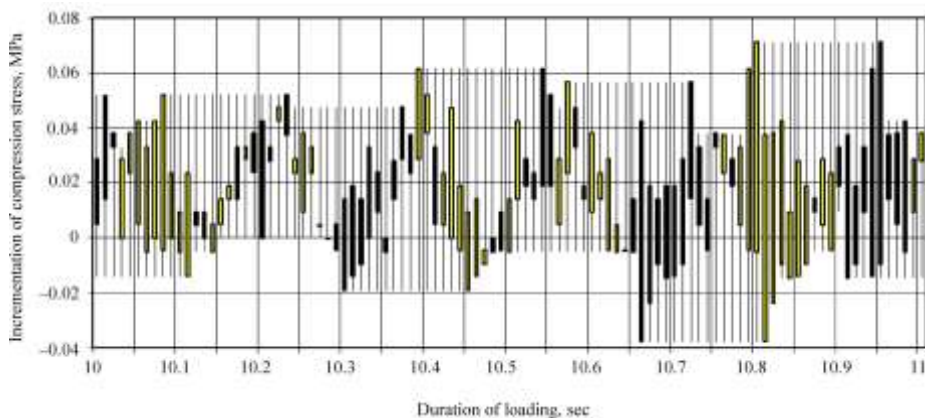
Table 2

Parameters of the fracture moment and the point of transition of the dispersal reinforced fine-grained concrete samples from the flat condition to the trend condition

Number of composition	Parameters of the fracture moment			Parameters of the transition point					
				absolute values			relative values		
	$t_{frac}, sec$	$\sigma_{comp}, MPa$	$\epsilon_{comp}, mm/m$	$t_{tz}, sec$	$\sigma_{tz}, MPa$	$\epsilon_{tz}, mm/m$	$\frac{t_{tz}}{t_{fr}}, \%$	$\frac{\sigma_{tz}}{\sigma_{comp}}, \%$	$\frac{\epsilon_{tz}}{\epsilon_{comp}}, \%$
1	21.1	29.03	1.234	11.52	16.07	0.667	54.59	55.35	54.07
2	20.34	28.58	1.215	5.92	5.40	0.345	29.11	18.91	28.42
3	21.23	23.90	1.278	10.08	10.42	0.600	47.48	43.60	46.95



a



b

Fig. 6. Analysis of vicinity of the point of transition from the flat to trend condition for the sample of the reference fine-grained concrete composition with the help of Japanese candlesticks charting (incrementation of compression stress)

last point of the interval. The rectangular candlestick body shows fluctuations of the parameter during the interval. The top of the shadow shows the maximum, and the lowest point shows the minimum in the time interval. If the candlestick body is black, we see decrease of the parameter. The white body means increase of the parameter.

Analyzing a range of fine-grained concrete compositions, we defined that the point of transition of the sample from a relatively quiescent flat condition to the trend condition in the vicinity of the point under  $\mu \approx 0,5$  follows the stage of stress incrementation decrease, for example, see the section of the deformation curve in the interval from 9.28 to 9.43 sec (Fig. 6, a). This situation speaks for certain difficulties during redistribution of stresses along the volume of the composite material, the process of structure decompaction and the beginning of the micro-fracturing process (the first parametric point, according to Berg). This stage is related to emergence of a dangerous active crack (the defect of the structure in the form of pores, openings or inclusions of the filler).

We can see the structuring growth of increase and decrease stages of stress incrementation with increase of the load in the interval from the transition point to the fracture point. We can explain discretization of stress increase and decrease under steady increase of the deformation and load received by the sample as well as growth of the order in the structuring of increase and decrease stages of stress increment on that stage by the discrete nature of cracks development that is shown by local propagation of the crack for the minimum critical length. Current time interval has the following specific: nonlinear nature of the deformation curve [1, 23], further development of the structure decompaction process, generation of local fracture nucleuses, generation of bifurcation points and the main crack up to fracturing of the sample.

It was discovered that the fine-grained concrete, containing 1.5 % of the high-modulus polyacrylic synthetic fiber FibARM Fiber WB in the binder mass, has the quickest generation process of the first critical condition. This condition is characterized by the stress up to 19 % of the bearing capacity and the ultimate deformation about 28 %. Appending 1 % of the low-modulus polypropylene multifilament fiber (the cut length of 12 mm, diameter of 25-35 micron) or 5 % of the astralene modified basalt microfiber Astroflex-MBM (the length of 100-500 micron, diameter of 8÷10 micron) leads to essential increase of the first critical level, around 54 and 47 % accordingly, during the analysis of both stress increment and deformations.

## Conclusion

The proposed methodology of the deformation curves fractal analysis on the basis of the minimal covering method and its implementation for compositions of dispersal reinforced fine-grained concrete allows to quantitatively define location of the parametric points that is an important informative characteristic for study of fracturing processes in composite materials of different nature. Deformation

curves tracing with the minimum step of reading " $\sigma - \varepsilon$ " and their fractal analysis from the perspective of dynamic series open up new opportunities to study fracture mechanics of construction composite materials.

## Acknowledgment

The reported study was funded by RFBR according to the research project № 18-29-12036.

## References

1. Berg O.Y., Shcherbakov E.N., Pisanko E.N. Vysokoprochnyj beton [High-strength concrete]. *Moskva: Sroyzdat*, 1971, 208 P
2. Zaycev Y.V. Modelirovanie deformacii i prochnosti betona metodami mehaniki razrusheniya [Modelling of deformation and strength of the concrete by methods fracture mechanics]. *Moskva: Sroyzdat*, 1982. 196 P.
3. Karpenko N.I. Obshhie modeli mehaniki zhelezobetona [General models of mechanics of reinforced concrete]. *Moskva: Sroyzdat*, 1996, 416 P.
4. Selyayev V.P. Fraktal'nye modeli razrusheniya betonov [Fractal models of destruction of concretes], *Regional'naja arhitektura i stroitel'stvo*. 2015, No 1, pp. 11-22.
5. Ivanova V.S., Balankin A.S., Bunin I.J., Oxogoev A.A. Sinergetika i fraktaly v materialovedenii [Synergetics and fractals in science of materials], *Moskva: Nauka*, 1994, 384 P.
6. Selyayev V.P., Nizina T.A., Lankina Y.A. Fraktal'nyj analiz struktury napolnennykh polimernykh kompozitov [Fractal analysis of the structure of filled polymer composites], *Izvestija VUZov. Stroitel'stvo*. 2007, No. 4, pp. 43-48.
7. Khahardin A.N., Khodykin E.I. Fraktal'naja razmernost' dispersnykh i poristykh materialov [Fractal dimension of dispersed and porous materials], *Stroitel'nye materialy*, 2007, No. 8, pp. 62-63.
8. Selyayev V.P., Nizina T.A., Lankina Y.A., Tsyganov V.V. Opredelenie fraktal'noj razmernosti kak strukturnogo parametra pri analize polimernykh kompozitov [Determination of fractal dimension as a structural parameter in the analysis of polymer composites]. *Dostizheniya, problemy i perspektivnye napravleniya razvitiya teorii i praktiki stroitel'nogo materialovedeniya: Desyatye Akademicheskie chteniya RAASN. – Kazan': Izd-vo KGASU*, 2006, pp. 73-76
9. Pertsev V.T. Topologicheskaja optimizacija processov formirovaniya mikrostruktury cementnogo kamnja i betona [Topological optimization of the processes of microstructure formation of cement stone and concrete], *Nauchnyj vestnik Voronezhskogo gosudarstvennogo arhitekturno-stroitel'nogo universiteta. Serija: Fiziko-himicheskie problemy i vysokie tehnologii stroitel'nogo materialovedeniya*, 2015, No. 1, pp. 21-28.
10. Hamidulina D.D., Shishkin I.V. Primenenie teorii fraktal'noj geometrii v stroitel'nom materialovedenii [Application of the theory of fractal geometry in building materials science], *Aktual'nye problemy sovremennoj nauki, tehniki i obrazovaniya*, 2015, Vol. 2, No. 1, pp. 5-8.
11. Bannikov M.V. Jeksperimental'noe issledovanie fraktal'nykh zakonov rosta ustalostnoj treshhiny i dissipacii jenerгии v ee vershine [Experimental study of fractal properties of fatigue crack growth and energy dissipation in crack tip], *Bulletin of PNRPU. Mechanics*, 2013, No. 2, pp. 21-36.
12. Oborin V.A., Bannikov M.V., Bayandin Y.V., Sokovikov M.A., Bilalov D.A., Naimark O.B. Fractal analysis of fracture surface of aluminum alloy AMg6 under fatigue and dynamic loading.

PNRPU Mechanics Bulletin. 2015. No. 2. Pp. 116-126. DOI: 10.15593/perm.mech/2015.2.07

13. Krivonosova E.K., Pervadchuk V.P. Ispol'zovanie fraktal'nogo podhoda dlja analiza stabil'nosti mnogourovnevnyh struktur [Fractal approach to the multilevel structure stability analysis], Vestnik PNIPU. Mashinostroenie, materialovedenie, 2013, No. 1(15), pp. 63–69.

14. Krivonosova E.A., Schicin Y.D., Krivonosova E.K. Fractal analysis of multilevel structure formation. *The International Symposium on visualization through advanced measurements and simulation.* – Osaka, 2014, pp. 287–289.

15. Maslovskaya A.G., Osokina A.G., Barabash T.K. Application of fractal methods to analysis dynamic data [Primenenie fraktal'nyh metodov dlja analiza dinamicheskikh dannyh]. Vestnik Amurskogo gosudarstvennogo universiteta, 2010, Vol. 51: Ser. Estestv. i jekon. nauki. pp. 13-20.

16. Vladimirova D.B. Indeks fraktal'nosti v issledovanijah determinirovannosti diskretnyh vremennyh rjadov [Index of fractality in the study of deterministic discrete time series]. Nauka i biznes: puti razvitiya. 2015. No. 8(50), pp. 86-91.

17. Feder E. Fraktaly: per. s angl [Fractals: translation from English]. Moskva: Mir, 1991, 254 P.

18. Mandelbrot B.B. The fractal geometry of nature. N.Y.: Freeman, 1983, 480 P.

19. Starchenko N.V. Indeks fraktal'nosti i lokal'nyj analiz haoticheskikh vremennyh rjadov: Dis. ... k-ta fiz.-mat. nauk: 01.01.03 [Index of fractality and local analysis of chaotic time series: Dissertation on competition of a scientific degree of candidate of physical and mathematical sciences: 01.01.03]. Moscow, 2005. 122 P.

20. Dubovikov M.M., Starchenko N.S. Variation index and its applications to analysis of fractal structures // Sci. Almanac Gordon. 2003. Vol. 1. P. 1-30.

21. Dubovikov M.M., Starchenko N.S., Dubovikov M.S. Dimension of the minimal cover and fractal analysis of time series // Physica. 2004. A 339. P. 591-608.

22. Nison S. [Japanese candlesticks: graphical analysis of financial markets. Translation from English. Dozorova T., Volkova M.M.: Publishing house «Diagram», 1998. 336 p. (rus)

23. Bondarenko V.M., Selyaev V.P., Selyaev P.V. Fizicheskie osnovy prochnosti betona [Physical basis of concrete strength], Beton i zhelezobeton. 2014. No. 4, pp. 2-5.